SLAC-PUB-13008
arXiv:0710/5207v1[astro-ph]

Birth of massive black hole binaries

By MONICA COLPI[1], MASSIMO DOTTI[2], LUCIO MAYER[3] AND STELIOS KAZANTZIDIS[4]

[(1)]Department of Physics G. Occhialini, University of Milano Bicocca, Milano, Italy, [(2)]Department of Physics, University of Insubria, Como, Italy, [(3)]Insitute of Theoretical Physics, Zurich, Switzerland, [(4)] Kavli Institute for Particle Astrophysics and Cosmology, Department of Physics, Stanford University, USA

If massive black holes (BHs) are ubiquitous in galaxies and galaxies experience multiple mergers during their cosmic assembly, then BH binaries should be common albeit temporary features of most galactic bulges. Observationally, the paucity of active BH pairs points toward binary lifetimes far shorter than the Hubble time, indicating rapid inspiral of the BHs down to the domain where gravitational waves lead to their coalescence. Here, we review a series of studies on the dynamics of massive BHs in gas-rich galaxy mergers that underscore the vital role played by a cool, gaseous component in promoting the *rapid formation of the BH binary*. The BH binary is found to reside at the center of a massive self-gravitating nuclear disc resulting from the collision of the two gaseous discs present in the mother galaxies. Hardening by gravitational torques against gas in this grand disc is found to continue down to sub-parsec scales. The eccentricity decreases with time to zero and when the binary is circular, accretion sets in around the two BHs. When this occurs, each BH is endowed with it own small-size ($\lesssim 0.01$ pc) accretion disc comprising a few percent of the BH mass. Double AGN activity is expected to occur on an estimated timescale of $\lesssim 1$ Myr. The double nuclear point–like sources that may appear have typical separation of $\lesssim 10$ pc, and are likely to be embedded in the still ongoing starburst. We note that a potential threat of binary stalling, in a gaseous environment, may come from radiation and/or mechanical energy injections by the BHs. Only short–lived or sub–Eddington accretion episodes can guarantee the persistence of a dense cool gas structure around the binary necessary for continuing BH inspiral.

1. Introduction

Dormant black holes (BHs) with masses in excess of $\gtrsim 10^6\,M_\odot$ are ubiquitous in bright galaxies today (Kormendy & Richstone 1995; Richstone 1998). Relic of an earlier active phase as quasars, these massive BHs appear a clear manifestation of the cosmic assembly of galaxies. The striking correlations observed between the BH masses and properties of the underlying hosts (Magorrian et al. 1998; Ferrarese & Merritt 2000; Gebhardt et al. 2000; Graham & Driver 2007) indicates unambiguously that BHs evolve in symbiosis with galaxies, affecting the environment on large–scales and self-regulating their growth (Silk & Rees 1998; King 2000; Granato et al. 2004; Di Matteo, Springel & Hernquist, 2005).

According to the current paradigm of structure formation, galaxies often interact and collide as their dark matter halos assemble in a hierarchical fashion (Springel, Frenk & White 2006), and BHs incorporated through mergers into larger and larger systems are expected to evolve concordantly (Volonteri, Haardt & Madau 2003). In this astrophysical context, close BH *pairs* form as natural outcome of binary galaxy mergers (Kazantzidis et al. 2005).

In our local universe, one outstanding example is the case of the ultra–luminous infrared galaxy NGC 6240, an ongoing merger between two gas–rich galaxies (Komossa et al. 2003; for a review on binary black holes see also Komossa 2006). *Chandra* images have revealed the occurrence of two nuclear X-ray sources, 1.4 kpc apart, whose spectral distribution is consistent with being two accreting massive BHs embedded in the diluted

Contributed to STScI Spring Symposium on Black Holes, 04/23/2007--4/26/2007, Baltimore, Maryland

Work supported in part by US Department of Energy contract DE-AC02-76SF00515

emission of a starburst. Similarly, Arp 299 (Della Ceca et al. 2002; Ballo et al. 2004) is an interacting system hosting an obscured active nucleus, and possibly a second less luminous one, distant several kpc away. A third example is the elliptical galaxy 0402+369 where the cleanest case of a massive BH *binary* has been recently discovered. Two compact variable, flat–spectrum active nuclei are seen at a projected separation of only 7.3 pc (Rodriguez et al. 2006). Arp 299, NGC 6240, and 0402+369 may just highlight different stages of the BH dynamical evolution along the course of a merger, with 0402+369 being the latest, most evolved phase (possibly related to a dry merger). Energy and angular momentum losses due to gravitational waves are not yet significant in 0402+392, so that stellar interactions and/or material and gravitational torques are still necessary to bring the BHs down to the domain controlled by General Relativity.

From the above considerations and observational findings, it is clear that binary BH inspiral down to coalescence is a major astrophysical process that can occur in galaxies. It is accompanied by a gravitational wave burst so powerful to be detectable out to very large redshifts with current planned experiments like the Laser Interferometer Space Antenna (*LISA*; Bender et al. 1994; Vitale et al. 2002). These extraordinary events will provide not only a firm test of General Relativity but also a view, albeit indirect, of galaxy clustering (Haehnelt 1994; Jaffe & Backer 2003; Sesana et al. 2005). With *LISA*, BH masses and spins will be measured with such an accuracy (Vecchio 2004) that it will be possible to trace the BH mass growth across all epochs. Interestingly, *LISA* will explore a mass range between $10^3\,M_\odot$ and $10^7\,M_\odot$ that is complementary to that probed by the distant massive quasars ($> 10^7\,M_\odot$), providing a complete census of the BHs in the universe.

Both minor as well as major mergers with BHs accompany galaxy evolution in environments that involve either gas-rich (wet) as well as gas-poor (dry) galaxies. Thus, the dynamical response of galaxies to BH pairing should differ in many ways according to their properties. Exploring the expected diversities in a self-consistent cosmological scenario is a major challenge and only recently, with the help of high-resolution N-body/SPH simulations, it has become possible to "start" addressing a number of compelling issues. Galaxy mergers cover cosmological volumes (a few to hundred kpc aside), whereas BH mergers probe volumes of only few astronomical units or less. Thus, tracing the BH dynamics with scrutiny requires N-Body/SPH force resolution simulations spanning more than nine orders of magnitude in length. For this reason, two complementary approaches have been followed in the literature. A statistical approach (based either on Monte Carlo realizations of merger trees or on N-Body/SPH large scale simulations) follows the collective growth of BHs inside dark matter halos. Supplemented by semi-analytical modeling of BH dynamics (Volonteri et al. 2003) or/and by sub-grid resolution criteria for accretion and feedback (Springel & Hernquist 2003; Springel, Di Matteo & Hernquist 2005), these studies have proved to be powerful in providing estimates of the expected coalescence rates, and in tracing the overall cosmic evolution of BHs including their feedback on the galactic environment (Di Matteo, Springel & Hernquist 2005; Di Matteo et al. 2007). The second approach, that we have been following, looks at individual binary collisions, as it aims at exploiting in detail the BH dynamics and some bulk physics from the galactic scale down to and within the BH sphere of influence. Both approaches, the collective and the individual, are necessary and complementary, the main challenge being the implementation of realistic input physics in the dynamically active environment of a merger.

Following a merger, how can BHs reach the gravitational wave inspiral regime? The overall scenario was first outlined by Begelman, Blandford & Rees (1980) in their seminal study on the dynamical evolution of BH pairs in pure stellar systems. They indicated

three main roots for the loss of orbital energy and angular momentum: (I) dynamical friction against the stellar background acting on each individual BH; (II) hardening via 3–body scatterings off single stars when the BH binary forms; (III) gravitational wave back–reaction.

Early studies explored phase (I) simulating the collisionless merger of spherical halos (Makino & Ebisuzaki 1996; Milosavljević & Merritt 2001; Makino & Funato 2004). Governato, Colpi & Maraschi (1994) in particular first noticed that when two equal mass halos merge, the twin BHs nested inside the nuclei are dragged effectively toward the center of the remnant galaxy by dynamical friction and form a close pair, but that the situation reverses in unequal mass mergers, where the less massive halo tidally disrupted leaves its "naked" BH wandering in the outskirts of the main halo. Thus, depending on the halo mass ratio and internal structure, the transition from phase (I) to phase (II) can be prematurely aborted or drastically relented. Similarly, the transit from phase (II) to phase (III) is not always secured, as the stellar content inside the "loss cone" may not be rapidly refilled with fresh low–angular momentum stars to harden the binary down to separations where gravitational wave driven inspiral sets in (see, e.g., Milosavljevic & Merritt 2001; Yu 2002; Berczik, Merritt & Spurzem 2005; Sesana, Haardt & Madau 2007). For an updated review on the last parsec problem and its possible solution (see Merritt 2006a; Gualandris & Merritt 2007).

Since BH coalescences are likely to be events associated with mergers of (pre–)galactic structures at high redshifts, it is likely that their dynamics occurred in gas dominated backgrounds, NGC 6240 being just the most outstanding case visible in our local universe. Other processes of BH binary hardening are expected to operate in presence of a dissipative gaseous component that we will highlight and study here.

Kazantzidis et al. (2005) first explored the effect of gaseous dissipation in mergers between gas–rich disc galaxies with central BHs, using high resolution N–Body/SPH simulations. They found that the merger triggers large–scale gas dynamical instabilities that lead to the gathering of cool gas deep in the potential well of the interacting galaxies. In minor mergers, this fact is essential in order to bring the BHs to closer and closer distances before the less massive galaxy, tidally disrupted, is incorporated in the main galaxy. Moreover, the interplay between strong gas inflows and star formation leads naturally to the formation, around the two BHs, of a grand, massive ($\sim 10^9\,\mathrm{M}_\odot$) gaseous disc on a scale smaller than $\sim$ 100 pc. It is in this equilibrium circum–nuclear disc that the dynamical evolution of the BHs continues, after the merger has been subsided. Escala et al. (2005, hereinafter ELCM05; see also Escala et al. 2004) have been the first to study the role played by gas in affecting the dynamics of massive ($\sim 10^8\,\mathrm{M}_\odot$) twin BHs in equilibrium Mestel discs of varying clumpiness. In both these approaches (i.e., in the large scale simulations of Kazantzidis et al., and in the equilibrium disc models of ELCM05) it was clear that the gas temperature is a key physical parameter and that a hot gas brakes the BHs inefficiently. Instead, when the gas is allowed to cool, the drag becomes efficient: the large enhancement of the local gas density relative to the stellar one leads to the formation of prominent density wakes that are decelerating the BHs down to the scale where they form a "close" binary. Later, binary hardening occurs under mechanisms that are only partially explored, and that are now subject of intense investigation. The presence of a cool circum–binary disc and of small–scale discs around each individual BH appear to be critical for their evolution down to the domain of gravitational waves driven inspiral. In this context there is no clear "stalling problem" that emerges from current hydrodynamical simulations but this critical phase need a more through, coherent analysis.

The works by Kazantzidis et al. (2005) and ELCM05 have provided our main motiva-

tion to study the process of BH pairing along two lines: In gas-rich binary mergers, line (1) aims at studying the transit from state (A) of pairing when each BH moves individually inside the time-varying potential of the colliding galaxies, to state (B) when the two BHs dynamically couple their motion to form a binary. The transit from (A) → (B) requires exploring a dynamic range of five orders of magnitude in length from the cosmic scale of a galaxy merger of 100 kpc down to the parsec scale for BHs of million solar masses (i.e., BHs in the LISA sensitivity domain). After all transient inflows have subsided and a new galaxy has formed, the BH binary is expected to enter phase (C) where it hardens under the action of gas-dynamical and gravitational torques. Research line (2) aims at studying the braking of the BH binary from (B) → (C) and further in, exploring the possibility that during phase (C) two discs form and grow around each individual BH. As first discussed by Gould & Rix (2000) the binary may later enter a new phase (D) controlled by the balance of viscous and gravitational torques in a circum–binary disc surrounding the BHs, in a manner analogous to the migration of planets in circum-stellar discs (a scenario particularly appealing when the BH mass ratio is less than unity). Phase (D) likely evolves into (E) when gravitational wave inspiral terminates the BH binary evolution.

There is a number of key questions to address:
(i) How does transition from state (A) → (B) depend on the gas thermodynamics? How do BHs bind?
(ii) In the grand nuclear disc inside the remnant galaxy, how do eccentric orbits evolve? Do they become circular or highly eccentric?
(iii) During the hardening through phase (B) and (C), do the BHs collect substantial amounts of gas to form cool individual discs?
(iv) Can viscous torques drive the binary into the gravitational wave decaying phase?
(v) Is there a threat of a *stalling* problem when transiting from (C) → (D) or from (D) → (E)? And, for which mass ratios and ambient conditions?

2. Dynamics of BHs in disc–galaxy mergers

In this section, we track the large–scale dynamics of two massive BHs during the merger between two gas–rich (equal mass) disc galaxies, and later focus on the process leading to the formation of a Keplerian BH binary.

2.1. *Modeling galaxy mergers*

We start simulating, with the N-Body/SPH code *Gasoline* (Wadsley, Stadel & Quinn 2004), the collision between two galaxies, similar to the Milky Way, comprising a stellar bulge, a disc of stars and gas, and a massive, extended spherical dark matter halo with NFW density profile (Navarro, Frenk & White 1996; Klypin, Zhao & Somerville 2002). The halo has a virial mass $M_{\rm vir} = 10^{12}\,{\rm M}_\odot$, concentration parameter $c = 12$ and dimensionless spin parameter $\lambda = 0.031$ consistent with current structure formation models. The disc of mass $M_{\rm disc} = 0.04 M_{\rm vir}$ has a surface density distribution that follows an exponential law with scale length of 3.5 kpc and scale height 350 pc. The spherical bulge (Hernquist 1993) has mass $M_{\rm bulge} = 0.008 M_{\rm vir}$ and scale radius of 700 pc. Initially, the dark matter halo has been adiabatically contracted to respond to the growth of the disc and bulge, resulting in a model with a central density slope close to isothermal. Each galaxy consists of 10^5 stellar disc particles, 10^5 bulge particles, and 10^6 halo particles. The gas fraction, $f_{\rm g}$, is 10% of the total disc mass and is represented by 10^5 particles (10^6 in a refined simulation). To each of the galaxy model we added a softened particle, initially at rest, to represent the massive BH at the center of the bulge. The BH mass is

$M_{\rm BH} = 2.6 \times 10^6 M_\odot$, according to $M_{\rm BH}$–σ relation. In the major merger, the BHs are twin BHs (i.e., the mass ratio $q_{\rm BH} = 1$).

Different encounter geometries were explored in the simulations by Kazantzidis et al. (2005): they comprise prograde or retrograde coplanar mergers as well as mergers with galactic discs inclined relative to the orbital plane. The simulation presented in this proceeding refers to a coplanar prograde encounter. This particular choice is by no means special for our purpose, except that the galaxies merge slightly faster than in the other cases thus limiting our computational burden. The galaxies approach each other on parabolic orbits with pericentric distances equal to 20% of the galaxy's virial radius, typical of cosmological mergers (Khochfar & Burkert 2006). The initial separation of the halo centers is twice their virial radii and their initial relative velocity is determined from the corresponding Keplerian point–mass orbit.

We include radiative cooling from a primordial mixture of hydrogen and helium, and adopt the star formation algorithm by Katz (1992) where gas particles, in dense cold Jeans unstable regions and in convergent flows, spawn N-body particles at a rate proportional to the local dynamical time (with star formation efficiency of 0.1). Radiative cooling is switch off at a relatively high floor temperature of 20,000 K to account for turbulent heating, non–thermal pressure forces, and the presence of a warm interstellar medium. In this large–scale simulation, the force resolution is ~ 100 pc.

The computational volume is later refined during the final stage of the merger with the technique of static particle splitting (Kaufmann et al. 2006) in order to achieve a resolution of 2 pc. The fine-grained region is large enough to guarantee that the dynamical timescale of the entire coarse-grained region is much longer than the dynamical timescale of the refined region so that gas particles from the coarse region will reach the fine region on a timescale longer than the actual time span probed in this work. In the refined simulations stars and dark matter particles essentially provide a smooth background potential, while the computation focuses on the gas component which dominates by mass in the nuclear region. A volume of 30 kpc in radius is selected while the two galaxy cores are separated by only 6 kpc. Inside this region, the simulation is carried on with as many as 2×10^6 gas particles. The mass resolution in the gas component, originally of $2 \times 10^4 M_\odot$, now becomes $\sim 3000 M_\odot$ after splitting.

A starburst with a peak star formation rate of $\sim 30\,{\rm M}_\odot\ {\rm yr}^{-1}$ takes place when the cores finally merge and it is in this environment that the BHs couple to form a binary. The short dynamical timescale involved in this process compared to the starburst duration ($\sim 10^8$ yr) suggest to model the thermodynamics and radiation physics simply via an effective equation of state. Calculations that include radiative transfer show that the thermodynamic state of a metal rich gas heated by a starburst can be approximated by an equation of state of the form $P = (\gamma - 1)\rho u$ with $\gamma = 7/5$ (Spaans & Silk 2000). The specific internal energy u evolves with time as a result of PdV work and shock heating modeled via the standard Monaghan artificial viscosity term. Shocks are generated even when a self-gravitating disc forms with strong spiral arms. The highly dynamical regime modeled here is different from that considered in the next section which could be evolved using an adiabatic equation of state. With this prescription we treat the gas as a one-phase medium whose mean density and internal energy (the sum of thermal and turbulent energy) correspond to the mean density and line width seen in observed nuclear discs (Downes & Solomon 1998).

2.2. *Large–scale dynamics and BH pairing*

The galaxies first experience few close fly-bys before merging. In these early phase of the collision, the cuspy potentials of both galaxies are deep enough to allow for the survival

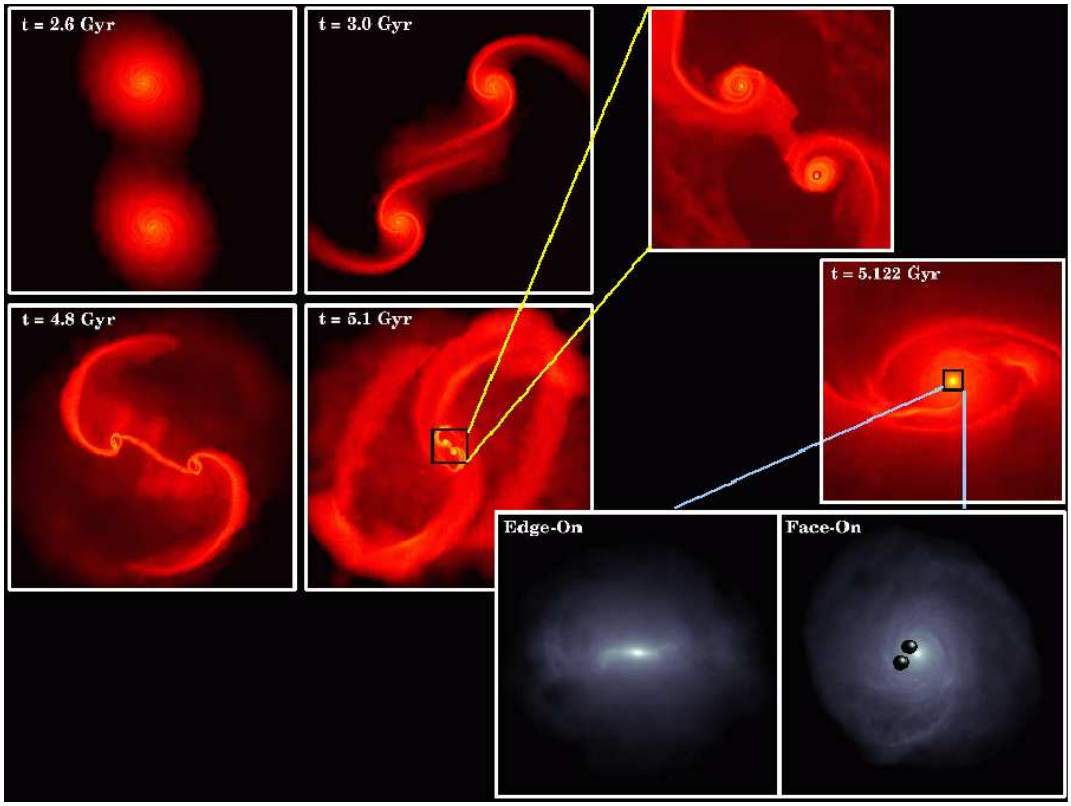

FIGURE 1. The different stages of the merger between two identical disc galaxies seen face–on. The color coded density maps of the gas component are shown using a logarithmic scale, with brighter colors for higher densities. The four panels to the left show the large-scale evolution at different times. The boxes are 120 kpc on a side (top) and 60 kpc on a side (bottom) and the density ranges between 10^{-2} atoms cm^{-3} and 10^{2} atoms cm^{-3}. During the interaction tidal forces tear the galactic discs apart, generating spectacular tidal tails and plumes. The panels to the right show a zoom in of the very last stage of the merger, about 100 million years before the two cores have fully coalesced (upper panel), and 2 million years after the merger (middle panel), when a massive, rotating nuclear gaseous disc embedded in a series of large-scale ring-like structures has formed. The boxes are now 8 kpc on a side and the density ranges between 10^{-2} atoms cm^{-3} and 10^{5} atoms cm^{-3}. The two bottom panels, with a gray color scale, show the detail of the inner 160 pc of the middle panel; the nuclear disc is shown edge-on (left) and face-on (right), and the two BHs are also shown in the face-on image.

of the baryonic cores where the BHs reside. As the two dark matter halos sink into one another under the action of dynamical friction, strong spiral patterns appear in both the stellar and the gaseous discs. Non–axisymmetric torques redistribute angular momentum, and as much as 60% of the gas originally present in the discs of the parent galaxies is funneled inside the inner few hundred parsecs of each core. This is illustrated in the upper right panel of Figure 1, where the enlarged color coded density map of the gas is shown, after 5.1 Gyr from the onset of the collision. *Each of the two BHs are found to be surrounded by a rotating stellar and gaseous disc of mass* $\sim 4\times10^{8}\ M_{\odot}$ *and size of a few hundred parsecs.* The two discs and BHs are just 6 kpc far apart. Meantime a starburst of $\sim 30\,\mathrm{M}_{\odot}\,\mathrm{yr}^{-1}$ has invested the central region of the merger.

It is tempting to imagine that an episode of accretion onto each BH starts at this time, similar to that observed in NGC 6240 (see Colpi et al. 2007, for a discussion on accretion

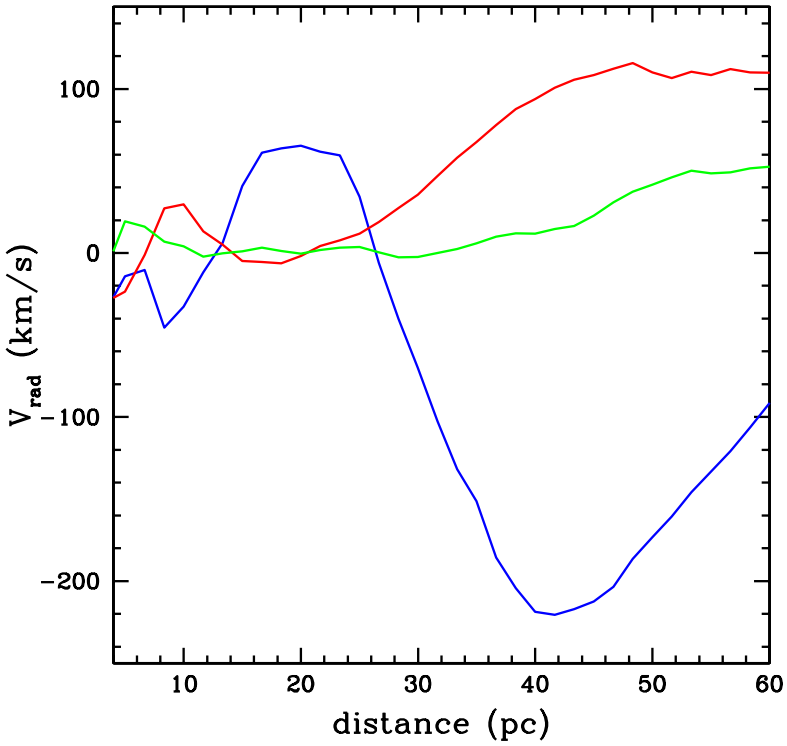

FIGURE 2. Radial velocities within the nuclear disc ($\gamma = 7/5$) starting at $t = 5.1218$ Gyr (blue line), and then after another 10^5 yr (red line) and 2×10^5 yr (green line). Remarkable inflow and outflow regions are the result of streaming motions within the bar and spiral arms arising in the disc during the phase of non-axisymmetric instability sustained by its self-gravity. At later times the instability saturates due to self-regulation, and the radial motions also level down (green line).

excited along the course of a large–scale merger). The *double* AGN activity in NGC 6240 occurs just on a similar scale, as the X–ray nuclei are 1 kpc apart in projection on the sky. It is remarkable that high–resolution near–infrared images at the Keck II telescope, combined with radio and X-ray positions, have revealed the habitat of the two active BHs in this ultra–luminous system. Each active BH appears to be at the center of a rotating stellar disc surrounded by a cloud of young star clusters lying in the plane of each disc (Max, Canalizo & de Vries 2007). This hints to a consumption of a fraction of the gas disc into stars along the course of the major merger and to BH fuelling by the winds of these young stars.

As the interaction proceeds in the simulation, the two baryonic discs around each BH get closer and closer, and eventually merge in a single structure: a massive circum–nuclear disc. This is illustrated in Figure 1, in the mid right panel. The two BHs are now at a relative separation comparable to the softening length of ~ 100 pc. At this stage we stop the simulation and start the one with increased resolution.

2.3. *Formation of a circum–nuclear disc*

The gaseous cores merge in a single nuclear disc with mass of $3 \times 10^9 M_\odot$ and size of $\lesssim 100$ pc. This *grand disc* is more massive than the sum of the two nuclear cores formed earlier

because radial gas inflows occur in the last stage of the galaxy collision. A strong spiral pattern in the disc produces remarkable radial velocities whose amplitude declines as the spiral arms weaken over time. Just after the merger, when non-axisymmetry is strongest, radial motions reach amplitudes of ~ 100 km s^{-1} (see Figure 2). This phase lasts only a couple of orbital times, while later the disc becomes smoother as spiral shocks increase the internal energy which in turn weakens the spiral pattern. Inward radial velocities of order $30 - 50$ km s^{-1} are seen for the remaining few orbital times. .

The disc is surrounded by several rings and by a more diffuse, rotationally-supported envelope extending out to more than a $\sim$ kpc from the center (Figure 1). A background of dark matter and stars distributed in a spheroid is also present but the gas component is dominant in mass within ~ 300 pc from the center.

The grand disc is rotationally supported ($v_{\rm rot} \sim 300$ km s^{-1}) and also highly turbulent, having a typical velocity $v_{\rm turb} \sim 100$ km s^{-1}. Multiple shocks generated as the cores merge are the main source of this turbulence. The disc is composed by a very dense, compact region of size about 25 pc which contains half of its mass (the mean density inside this region is $> 10^5$ atoms cm^{-3}). The outer region instead, from 25 to 75-80 pc, has a density 10-100 times lower, and is surrounded by even lower–density rotating rings that extend out to a few hundred parsecs. The disc scale height also increases from inside out, ranging from 20 pc to nearly 40 pc. The volume-weighted density within 100 pc is in the range $10^3 - 10^4$ atoms cm^{-3}, comparable to that of observed nuclear disc (Downes & Solomon 1998). This suggests that the degree of dissipation implied by our equation of state is a reasonable assumption despite the simplicity of the thermodynamical scheme adopted.

2.4. *Birth of a BH binary*

The BHs have been dragged together with their cores toward the dynamical center of the merging galaxies under the action of dynamical friction, and now move inside the grand disc.

They keep sinking down from about 40 pc to a few pc, our resolution limit. We find that *in less than a million years after the merger, the two holes are gravitationally bound to each other, as the mass of the gas enclosed within their separation is less than the mass of the binary. It is the gas that controls the orbital decay, not the stars.* Dynamical friction against the stellar background would bring the two BHs this close only on a much longer timescale, $\sim 5 \times 10^7$ yr (Mayer et al. 2007, supporting online material). This short sinking timescale comes from the combination of (1) the fact that gas densities are much higher than stellar densities in the center, and (2) that in the mildly supersonic regime the drag against a gaseous background is stronger than that in a stellar background with the same density (Ostriker 1999). Adding star formation is unlikely to change this conclusion as in our low-resolution galaxy merger simulations, the starburst timescale of $\sim 10^8$ yr is much longer than the binary formation timescale.

2.5. *Effect of thermodynamics of the BH sinking*

We tested how a smaller degree of dissipation in the gas affects the structure and dynamics of the nuclear region by increasing γ to 5/3. This would correspond to a purely adiabatic evolution. The radiative injection of energy from an active nucleus is a good candidate for a strong heating source that our model does not take into account (Spaans & Silk 2000; Klessen, Spaans & Jappsen 2007). An AGN would not only act as a source of radiative heating but would also increase the turbulence in the gas by injecting kinetic energy (Springel, Di Matteo & Hernquist 2005) in the surrounding medium, possibly

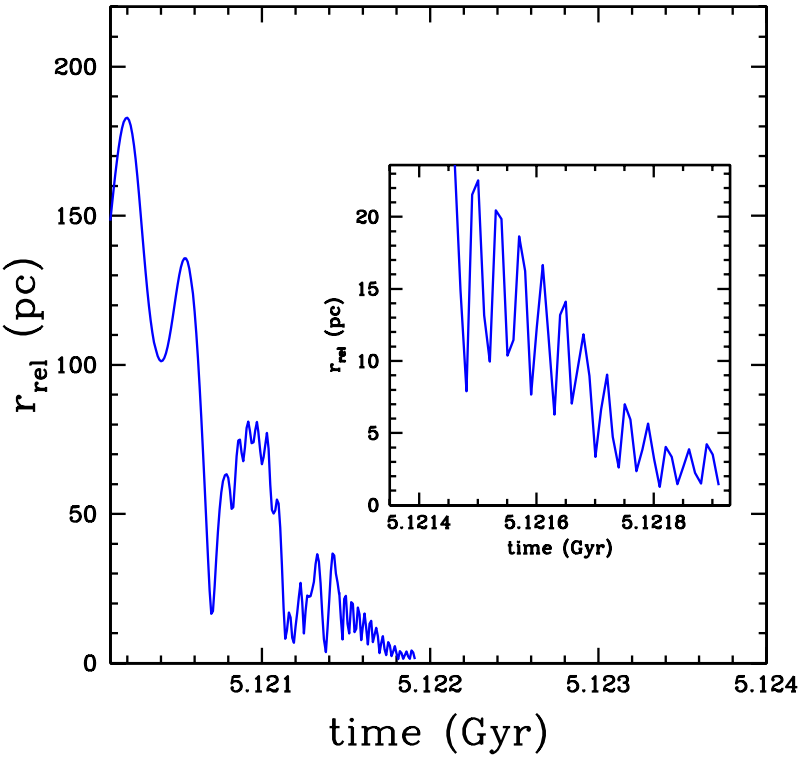

FIGURE 3. Orbital separation of the two BHs as a function of time during the last stage of the galaxy merger shown in Figure 1. The orbit of the pair is eccentric until the end of the simulation. The two peaks at scales of tens of parsecs at around $t = 5.1213$ Gyr mark the end of the phase during which the two holes are still embedded in two distinct gaseous cores. Until this point the orbit is the result of the relative motion of the cores combined with the relative motion of each BH relative to the surrounding core, explaining the presence of more than one orbital frequency. The inset shows the details of the last part of the orbital evolution, which takes place in the nuclear disc arising from the merger of the two cores. The binary stops shrinking when the separation approaches the softening length (2 pc).

suppressing gas cooling. Before the two galaxy cores merge, double (or single) AGN activity can in principle alter the thermal state of the gas.

We have run another refined simulation with $\gamma = 5/3$ to explore this extreme situation. In this case we find that a turbulent, pressure supported cloud of a few hundred parsecs arises from the merger rather than a disc. The mass of gas is lower within 100 pc relative to the $\gamma = 7/5$ case because of the adiabatic expansion following the final shock at the merging of the cores. The nuclear region is still gas dominated, but the stars/gas ratio is > 0.5 in the inner 100 pc. This suggests that the $\gamma = 5/3$ simulation does not describe the typical nuclear structure resulting from a dissipative merger.

The BH duet does not form a binary owing to inefficient orbital decay, and maintains a separation of $\sim 100 - 150$ pc, as shown in Figure 4. The gas is hotter and more turbulent; the sound speed $c_{\rm s} \sim 100$ km s^{-1} and the turbulent velocity $v_{\rm turb} \sim 300$ km s^{-1} are of the same order of $v_{\rm BH}$, the velocity of the BHs, and the density around them is ~ 5 times lower than in the $\gamma = 7/5$ case. Stars and gas will drive the BHs closer to form a

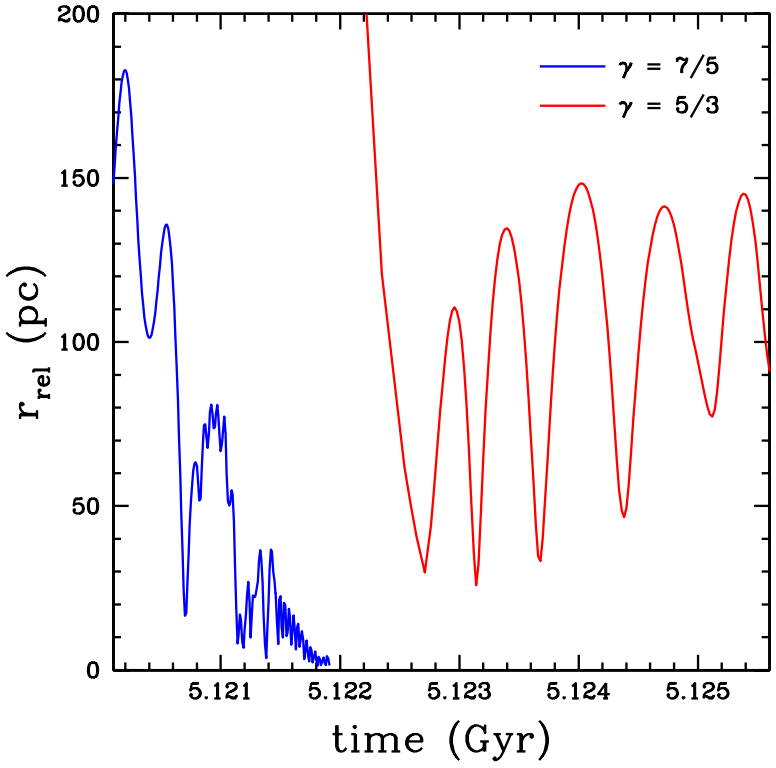

FIGURE 4. Orbital separation of the binary BHs. The blue line shows the relative distance as a function of time for $\gamma = 7/5$ as shown in Figure 2, while the red line shows it for $\gamma = 5/3$

binary, but on an estimated dynamical friction time of several 10^7 yr (Mayer et al. 2007, supporting online material).

3. BH inspiral in equilibrium rotating nuclear discs

3.1. *Initial conditions*

In this section, we present an independent series of simulations (carried out with *GADGET*; Springel, Yoshida & White 2001) that trace the dynamics of a BH pair (with $q_{\rm BH} = 1, 1/4, 1/10$) orbiting inside a self-gravitating, rotationally supported disc composed either of gas, gas and stars, or just stars (Dotti, Colpi & Haardt 2006; Dotti et al. 2007). The main parameters of the simulations are summarized in Table 1.

In all the simulations there are two BHs, a stellar bulge, and a massive rotationally supported nuclear disc composed by stars, gas, or both (except A3). The disc has a mass $M_{\rm Disc} = 10^8\,{\rm M}_\odot$, an extension of 100 pc, a vertical thickness of 10 pc, and follows a Mestel surface density profile:

$$\Sigma_{\rm Disc}(R) = \frac{K_{\rm Disc}}{R}, \tag{3.1}$$

where R is the radial distance projected into the disc plane, and $K_{\rm Disc}$ is determined by the total mass of the disc. The vertical profile of the disc is initially set homogeneous. The rotational velocity of the gas $v_{\rm rot}$ is constant through the disc and this implies that fluid elements are rotating differentially with an angular velocity $\Omega_{\rm rot} = v_{\rm rot}/R$. The

TABLE 1. Run parameters

run	central BH	f_*^a	$M^b_{\rm BH,1}$	$M^b_{\rm BH,2}$	$M^b_{\rm Disc}$	$M^b_{\rm Bulge}$	e	Q	res^c
A1					100		0		
A2	no	0	1	1	100	698	0.9	1.8	1
A3					0		0.9		
B1							0		
B2	no	0	5	1	100	698	0.9	1.8	1
B3^d							0.9		
C1^e				4					
C2	yes	0	4	1	100	698	0.7	3	1
C3				0.4					
D1				4					
D2	yes	1/3	4	1	100	698	0.7	3	1
D3				0.4					
E1				4					
E2	yes	2/3	4	1	100	698	0.7	3	1
E3				0.4					
F1				4					
F2	yes	1	4	1	100	698	0.7	3	1
F3				0.4					
G1^f	yes	0	4	4	100	698	0.4	3	0.1

[a] f_*: disc mass fraction in stars.
[b] BH masses are in units of 10^6 $M_\odot$.
[c] Force resolution in pc.
[d] The secondary lighter BH in run B3 has a retrograde orbit.
[e] simulation C1 was run two times, setting the secondary BH on a prograde and a retrograde orbit.
[f] Simulation C1 re–run using the particle splitting technique to improve force resolution.

spheroidal stellar bulge is modeled with 10^5 collisionless particles, initially distributed as a Plummer sphere with mass density profile:

$$\rho_{\rm Bulge}(r) = \frac{3}{4\pi}\frac{M_{\rm Bulge}}{b^3}\left(1+\frac{r^2}{b^2}\right)^{-5/2}, \qquad (3.2)$$

where b (= 50 pc) is the core radius, r the radial coordinate, and $M_{\rm Bulge}(= 6.98 M_{\rm Disc})$ the total mass of the spheroid. With such choice, the mass of the bulge within 100 pc is 5 times the mass of the disc, as suggested by Downes & Solomon (1998). We relax our initial composite model (bulge, disc and, if present, the central BH) for ≈ 3 Myrs, until the bulge and the disc reach equilibrium. Given the initial homogeneous vertical

structure of the disc, the gas initially collapses on the disc plane exciting small waves that propagate through the system. The parameters varying in the simulations are:
• The disc mass fraction in stars. We run four different sets of simulations assuming a purely gaseous disc (runs A, B, C, and G), and a disc in which 1/3 (runs D), 2/3 (runs E), and, finally, all gas particles (runs F) are turned into collisionless particles, respectively. For each disc model with fixed star fraction, we evolved the initial condition in isolation until equilibrium is reached. We do not convert any gaseous particle in stars when we follow the dynamics of the BHs, so that the disc stellar fraction remains constant;
• The disc mass. In all the simulations the disc mass is $\mathrm{M_{Disc}} = 10^8\,\mathrm{M_\odot}$, apart from run A3, in which we study the BH pair evolution in a pure stellar bulge.
• The Toomre parameter Q of the disc. In our simulations with a pure gaseous disc (runs A, B, C, and G), we set a initial internal energy profile $u(R) = K_{\rm Th}\ R^{-2/3}$, where $K_{\rm Th}$ is a constant defined so that the Toomre parameter of the disc,

$$Q = \frac{k c_{\rm s}}{\pi G \Sigma} \tag{3.3}$$

is $\gtrsim$1.8 for runs A and B (cold disc runs), and $\gtrsim$3 for runs C and G (hot disc runs) everywhere. In equation (3.3), k is the local epicyclic frequency and $c_{\rm s}$ is the local sound speed of the gas. The internal energy of the gas is evolved adiabatically neglecting radiative cooling/heating processes. Our choice of $Q > 1.8$ everywhere prevents fragmentation of the disc, and, when $Q > 3$ formation of large–scale over-densities, such as spiral arms or bars. We do not model any turbulent motion in the disc, but we consider the internal energy as a form of unresolved turbulence, and, as a consequence, $c_{\rm s}$ as local turbulent velocity. In the simulations with a non–null stellar fraction of the disc mass (runs D, E, and F) we set the local velocity dispersion of the disc stars equal to the local sound speed. With this procedure Q is the same than in a pure gaseous disc.
• The masses of the two BHs. As shown in Table 1, we explore various mass ratios $q_{\rm BH}$ from 1 to 1/10.
• The BH orbits. The BHs are placed on coplanar orbits that can either be prograde or retrograde, circular or eccentric (with e=0.4,0.7,0.9). In run A and B the two BHs are placed at 55 pc from the dynamical center of the disc. In run C,D,E,F the primary BH is at the center of the disc.
• The initial eccentricity of the orbiting BH. In all the runs of A and B classes a BH is initially moving on a circular orbit, while the second BH can have an orbital eccentricity (e) of 0 (circular motion, runs A1 and B1) or 0.9. In runs C, D, E, F, and G a BH is initially placed at rest in the center of the structure (see point 1) while the orbiting BH is initially moving on eccentric orbits with $e = 0.7$ in runs C, D, E, and F, $e = 0.4$ in run G1;
• The spatial resolution of the simulations. In our low resolution simulations (runs A, B, C, D, E, and F), we model our relaxed Mestel disc with 235331 particles, and use a number of neighbors of 50. This number defines a subsample of particles used by the code to evaluate the local hydrodynamical parameters. This number define, in the center of the disc, a hydrodynamical force resolution (usually defined as smoothing length) of $\approx$ 1 pc. We set also equal to 1 pc our gravitational softening, the parameter setting the spatial resolution of the gravitational acceleration evaluation. Evaluating the two forces, hydrodynamical and gravitational, with the same resolution prevents spurious local condensation of gas (occurring when the smoothing length exceeds the gravitational softening) or outflows (in the opposite case). The stellar gravitational softening is set equal to the gaseous one. In our high resolution simulation (run G1) we re-sample the output of simulation C1 thanks to the technique of particle splitting (Kitsionas & Whit-

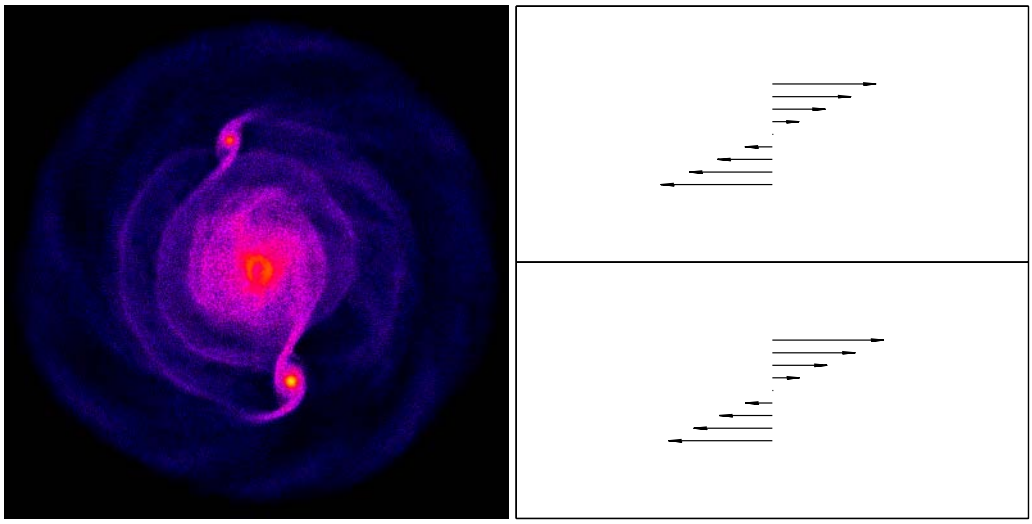

FIGURE 5. Left panel: face–on projection of the disc for run B1 at time 1 Myr. The color coding shows the z–averaged gas density on a logarithmic scale between 100 (dark blue) and 3×10^5 $M_\odot$ pc^{-3} (yellow). The two orbiting bright dots highlight the position of the two BHs (the top BH is the lighter one) theta are moving counterclockwise. They excite prominent wakes along their trails. Right panels: relative angular velocity pattern between the BHs and the gaseous disc for different radii. The upper(lower)–right panel is centered in the upper (lower) BH radius. The separations between two arrows are 1 pc.

worth 2002). With this technique we locally increase the number of gaseous particles of one order of magnitude reducing accordingly the smoothing length and the gravitational softening. The new spatial resolution in the central regions is 0.1 pc.

3.2. *Orbital decay on circular orbits*

In simulations A1 and B1, the BHs move initially on circular prograde orbits inside the disc. The initial separation, relative to the center of mass, is ≈ 55 pc.

We plot in Figure 5 the density map of the gas surrounding the unequal mass BHs in run B1 at a selected time. Both BHs are exciting prominent density wakes whose extent depends on the amount of disc mass perturbed by the orbiting BHs, which is a function of the BH masses, as can be noted in the Figure. The presence of two wakes near each BH is due to the different angular velocity pattern of the gas in the disc. Given our choice for the bulge and disc profile, in the BH comoving frame, the disc inside the BH orbit is moving counterclockwise while the outer regions are moving clockwise, as shown in the right panel of Figure 5. In a non rotating frame, two wakes develop around each BH, one outside the orbit and one inside. The motion of the BH is highly supersonic, and this explains the coherent structure and shape of their wakes (Ostriker 1999). The interaction between the BH and it inner wake increases the BH angular momentum, while the outer brakes the motion. Given our choice of the density/internal energy profiles, and the velocity field in the disc, the outer wake is more effective in removing orbital energy and angular momentum from each BH compared to the positive (accelerating) torque exerted by the wake excited in the inner part of the disc. The net effect is the braking of the BH pair, so that a binary can form on a timescale of $\sim 10^7$ yr.

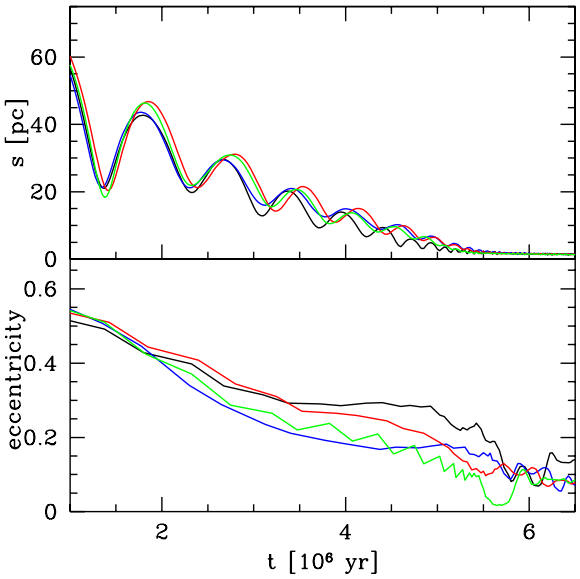

FIGURE 6. Equal mass BHs. Upper panel: separations s (pc) between the BHs as a function of time. Lower panel: eccentricity of the BH binary as a function of time. Black, blue, red and green lines refer to stellar to total disc mass ratio of 0, 1/3, 2/3 and 1 (run C1, D1, E1, and F1) respectively.

3.3. *Orbital decay along eccentric orbits*

Figure 6 shows the BH relative separation s and eccentricity as a function of time (upper and lower panel respectively) for equal mass, initially eccentric binaries of runs C1, D1, E1, and F1, where a primary BH is initially at rest in the dynamical center of the disc. Regardless the fraction of star–to–gas disc particles, the secondary BH spirals in, at the same pace, reaching $\sim$ 1 pc after $\sim$ 5 Myr. The velocity dispersion of the disc–stars is similar to the gas sound speed, and the two components share the same differential rotation. This is why dynamical friction on the secondary BH, caused by stars and gas, is similar. As the orbit decays, the eccentricity decreases to $e \lesssim 0.2$. This value is not a physical lower limit, but rather a numerical artifact due to the finite resolution, as will be shown in run G1.

Here, we show that circularization occurs regardless the nature of the disc particles (gas and/or stars). Note that circularization takes place well before the secondary feels the gravitational potential of the primary, so the BH mass ratio does not play any role in the process.

To show how the circularization process works, let us consider two different snapshot of run C1. In Figure 7 we plot the gas densities in the disc at the time corresponding to the first passage at the apocentre. In this simulation, the initially orbiting BH is corotating with the disc, with a speed equal, in modulus, to the velocity corresponding to a circular orbit at that initial position, but with an orbital eccentricity of 0.7. Near the apocenter the BH is moving slowlier than the gas in the disc, as highlighted by the two vectors in Figure 7, and in a frame comoving with the BH, gas blows ahead of the BH. The gas average rotational velocity decreases due to the gravitational interaction with the BH, and the back–reaction on the BH is a temporary "increase" of its orbital energy and

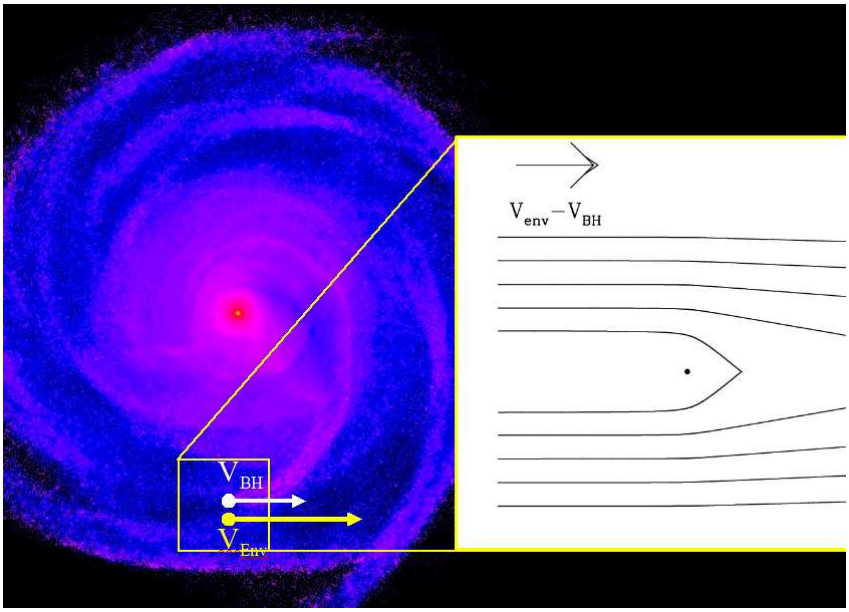

FIGURE 7. Face–on projection of the disc for run C1 at the first (co-rotating) BH apocentre. The color coding shows the z–averaged gas density, the white and yellow arrows refers to the BH and disc velocities, respectively. In the insert panel the trajectories of the gas particles are drawn, as observed in a frame comoving with the orbiting BH. The density wake is in front of the BH trail.

angular momentum. This excites a wake in the forward direction, i.e., at the apocenter the density wake is in front of the BH, as shown in Figure 7.

In Figure 8 we plot the gas densities in the disc at the time corresponding to the first passage at the pericenter. The BH has there a velocity higher than the local rotational velocity, so that dynamical friction causes a drag, i.e. a reduction of the BH velocity. Now, a wake of particles lags behind the BH trail. Thus, given this velocity difference, the wake reverses its direction decelerating tangentially the BH. Now the wake is behind the BH direction of motion. The orbital energy decreases more effectively than angular momentum, since at pericenter the gas density is also higher than at apocenter. The overall effect is a net circularization of the orbit. This seems a generic feature of dynamical friction, regardless the disc composition, and holds as long as the rotational velocity of the gas or/and star particles exceeds the gas sound speed and the stellar velocity dispersion, as in all cases explored. We remark that in spherical backgrounds, dynamical friction tends to increase the eccentricity, both in collisionless (Colpi, Mayer & Governato 1999; van den Bosch et al. 1999; Arena & Bertin 2007) as well as in gaseous (Sanchez–Salcedo & Brandenburg 2001) environments.

The interaction between the BH and the disc for counter–rotating orbits (run B3) keeps the BH orbit eccentric. When a counter–rotating BH is near apocenter, the gas flows against the BH motion. The over-density that forms is behind the BH trail, and this occurs also near pericenter. Dynamical friction is weaker than for co-rotating orbits given the larger relative velocity between the BH and the gas; thus the corresponding decay timescale is longer (by a factor ~ 2).

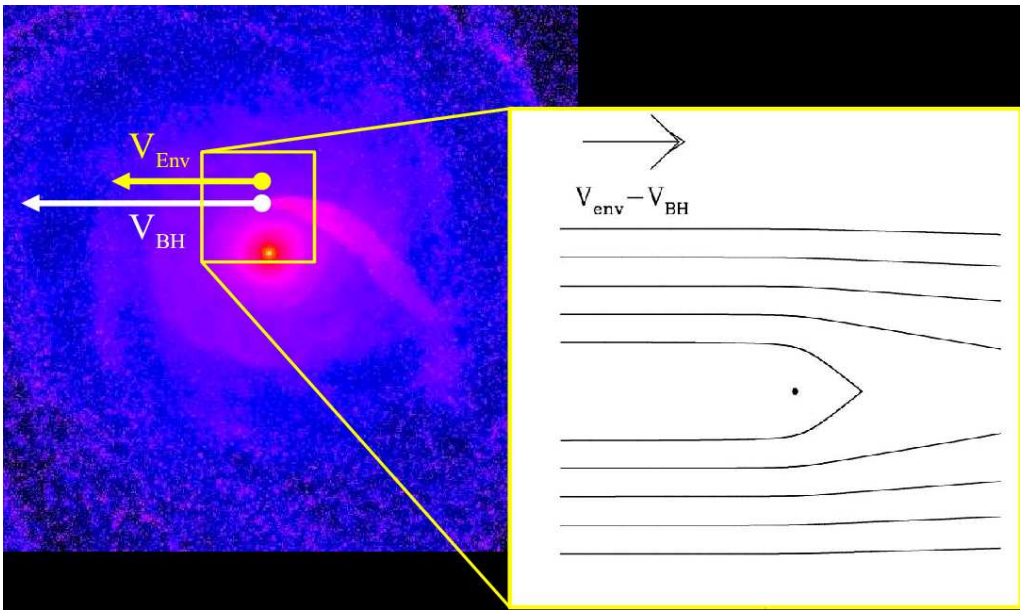

FIGURE 8. Same as Figure 7, but when the BH is at its first pericenter. The density wake is behind the BH trail.

3.4. *High resolution run: dynamics*

We run a higher resolution simulation to study the eccentricity and orbital evolution on scales smaller than 1 pc. The new initial condition is obtained re-sampling the output of run C1 (for equal mass BHs) with the technique of particle splitting. Re-sampling is performed when the BH separation is $\simeq 14$ pc (corresponding to $\simeq 4$ Myr after the start of the simulation). Splitting is applied to all particles whose distance from the binary center of mass is $\leqslant 42$ pc, so that the total number of particles increases only by a factor $\simeq 4$, while the local mass resolution in the split region is comparable to that of a standard $\simeq 2 \times 10^6$ particle simulation with uniform resolution. Our choice of the maximum distance for splitting is conservative, since it is aimed at preventing that more massive, unsplit gas particles reach the binary on a timescale shorter than the entire simulation time. In the central split region, the high mass resolution achieved fulfills the Bate & Burkert (1997) criterion for gravitational softening values down to 0.1 pc.

In Figure 9 we compare the surface density profile of the circum–nuclear gaseous disc in run C1 at $t = 4$ Myr, for the low and high resolution cases. The two profiles differ only below the scale of the low resolution limit $R \lesssim 3$ pc. The decrease of the gravitational softening corresponds to introducing a deeper potential well of the BH within a sphere defined by the former softening radius. Therefore, with the improved resolution, the central surface density increases as the gas reaches a new hydrostatic equilibrium closer to the BH, as shown in Figure 9 (red line). The lack of noticeable differences in the surface profile at separations $R > 3$ pc confirms the accuracy of the particle splitting technique.

Results of the high resolution run are shown in Figure 10. The separation decays down to 0.1 pc in ~ 10 Myr. In the high resolution run, the dynamical evolution of the BHs is initially identical to the low resolution case. Because of particle splitting, the system granularity is reduced, and therefore the force resolution increases. In the high resolution

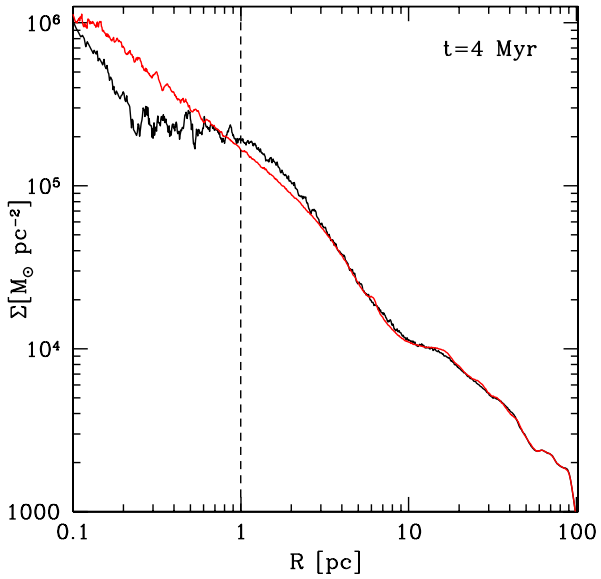

FIGURE 9. Surface density profile of the circum–nuclear gaseous disc in run C1 at $t = 4$ Myr. Black line refers to the surface density in the low resolution simulation, red line refers to the high resolution (split) simulation. The dashed vertical line marks the resolution limit in the un–split simulation.

run, the binary decreases its eccentricity to ≈ 0 (before the new spatial resolution limit is reached).

3.5. *High resolution runs: constrains on accretion processes*

In run G1, a resolution of 0.1 pc allows us to study the properties of the gas bound to each BH. To this purpose, it is useful to divide gaseous particles, bound to each BH, into three subsets, according to their total energy relative to the BH. We then define weakly bound (WB), bound (B), and strongly bound (SB) particles according to the following rule:

$$E < \begin{cases} 0 & \text{(WB)} \\ 0.25\,W & \text{(B)} \\ 0.5\,W & \text{(SB)}, \end{cases} \tag{3.4}$$

where E is the sum of the kinetic, internal and gravitational energy (per unit mass), the latter referred to the gravitational potential W of each individual BH. Hereafter WBPs, BPs, and SBPs will denote particles satisfying the WB, B, or SB condition, respectively. Note that, with the above definition, SBPs are a subset of BPs, which in turn are a subset of WBPs.

We find that the mass collected by each BH, relative to WB, B, and SB particles is $M_{\rm WBP} \approx 0.85 M_{\rm BH} \approx 3.4 \times 10^6\,{\rm M}_\odot$, $M_{\rm BP} \approx 0.41 M_{\rm BH} \approx 1.6 \times 10^6\,{\rm M}_\odot$, and $M_{\rm SBP} \approx 0.02 M_{\rm BH} \approx 8 \times 10^4\,{\rm M}_\odot$, respectively (here $M_{\rm BH} = M_1 = M_2$). These masses are remain constant with time as long as the BH separation is $s \gtrsim 1$ pc. At shorter separations WBPs and BPs are perturbed by the tidal field of the BH companion, and at the end of the simulation $M_{\rm WBP}$ and $M_{\rm BP}$ are reduced of a factor ≈ 0.1. During the same period of time, $M_{\rm SBP}$ associated to the primary (secondary) BH increases by a factor ≈ 4 (≈ 2.5). This

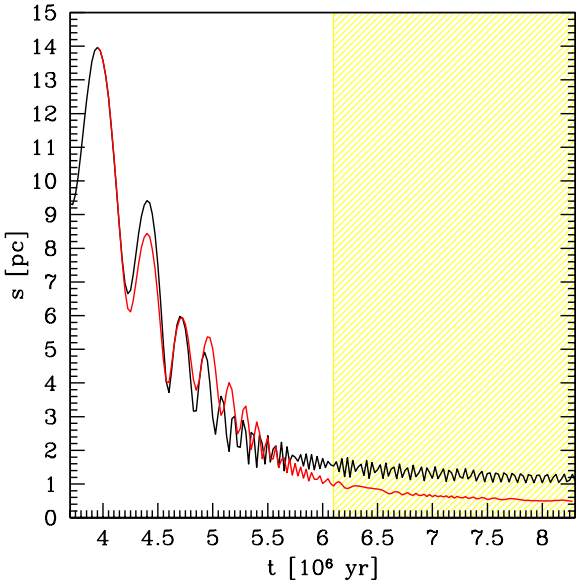

FIGURE 10. Separations s (pc) between the BHs as a function of time. Red (black) line refers to the (un–)split run C1. The dashed area corresponds to the region where the BH separation is < 1 pc in the split higher resolution.

result is unaffected by numerical noise since the number of bound particles (associated to each class) is $\gtrsim$1 SPH kernel ($N_{\rm neigh} = 50$).

The radial density profiles of WBPs, BPs, and SBPs are well resolved during the simulation. Bound particles have a net angular momentum with respect to each BH, and form a pressure supported spheroid. The half–mass radius is similar for the two BHs: $\simeq 3$ pc, $\simeq 1$ pc, and $\simeq 0.2$ pc for WBPs, BPs, and SBPs, respectively. The disc gas density can be as high as 10^7 cm^{-3}. It is then conceivable that, at these high densities, dissipative processes could be important, possibly reducing the gas internal (turbulent and thermal) energy well below the values adopted in our simulations. If cooling becomes effective, we expect that the bound gas will form a geometrically thin disc with Keplerian angular momentum comparable to what we found in our split simulation. Since $L_{\rm z} = \sqrt{G\,M_{\rm BH}\,R_{\rm BH,disc}}$, we obtain, for the primary BH, an effective radius $R_{\rm BH,disc} \approx 0.1$ pc (0.03 pc) for WBPs (BPs). The secondary BH is surrounded by particles with a comparatively higher angular momentum with a corresponding effective radius $R_{\rm BH,disc} \approx 1$ (0.13) pc for WBPs (BPs). Finally, for SBPs, both BHs have $R_{\rm BH,disc} \ll 0.01$ pc, which is more than an order of magnitude below our best resolution limit. These simple considerations indicate that a more realistic treatment of gas thermodynamics is necessary to study the details of gas accretion onto the two BHs during the formation of the binary, and the subsequent orbital decay. Nonetheless, our simplified treatment allows us to estimate a lower limit to the accretion timescale, assuming Eddington limited accretion:

$$t_{\rm acc} = \frac{\epsilon}{1-\epsilon}\, t_{\rm Edd}\, \ln\left(1 + \frac{M_{\rm acc}}{M_{\rm BH,0}}\right), \tag{3.5}$$

where ϵ is the radiative efficiency, $t_{\rm Edd} = c\sigma_T/(4\pi G m_{\rm p})$ the Salpeter time, σ_T the Thompson cross section, $M_{\rm BH,0}$ the initial BH mass, and $M_{\rm acc}$ the accreted mass. Assuming

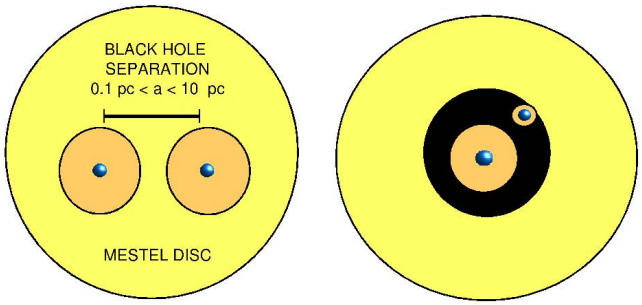

FIGURE 11. Left: a cartoon depicting the BH binary when the BH separation is $\gtrsim$0.1 pc, as suggested by our high-resolution simulation. The BHs are surrounded by their own accretion discs. Further orbital decay by gravitational and viscous torques are expected to open a gap leading to the configuration depicted in the right panel.

$\epsilon = 0.1$, Eddington limited accretion can last for ~ 15 Myr, and only $\lesssim$1 Myr, if the BHs accrete all the BPs, and SBPs, respectively.

Figure 11 depicts, in a cartoon, the configuration of the two accretion discs surrounding the BHs inside the grand disc. It is expected that the two discs will eventually touch and disrupt tidally, and re-organize to form a circum–binary geometrically thin disc surrounding both BHs; exploring this configuration is the goal of our next series of simulations. Further braking of the BH motion and binary hardening requires energy loss and angular momentum transport through a mechanism that may be reminiscent of planet migration in proto-stellar discs (Gould & Rix 2000): while gravitational torques carry away angular momentum, viscous torques inside the cool Keplerian circum–binary disc sustain the radial motion of the gas toward the BHs maintaining the binary in near contact with the disc. Equilibrium between the gravitational and viscous torques cause the slow drift of the BHs toward smaller and smaller separations until the gravitational waves guide final inspiral.

4. BH binaries, the $M_{\rm BH}$ versus σ relation and the stalling problem

In the previous section, we followed the orbital decay of a BH binary in a rotationally supported gaseous background, down to a scale of ~ 0.1 pc, and found that the hardening of the BH binary, and thus the corresponding energy and angular momentum loss, results from large–scale density perturbations excited by the BH gravitational. These perturbations have still negligible impact on the overall structure of the Mestel disc: compared with the binding energy of the disc, the energy deposited by the BH binary is still small ($\approx$ an order of magnitude lower). But this may not hold true if the binary continues to harden down to the scale where gravitational wave emission becomes important. Unless gravitational torques are capable of extracting angular momentum with no

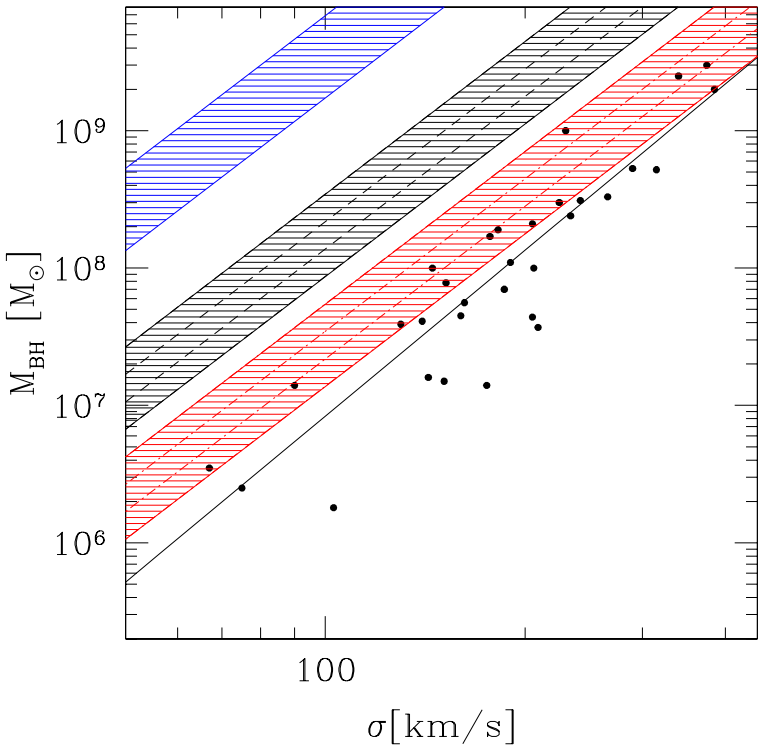

FIGURE 12. $M_{\rm BH}$–σ plane: thin solid line is the best fit to the data (Tremaine et al. 2002). Black (blue) lines refer $M_{\rm BH}^{\rm max} \equiv \mathcal{M}(t_{\rm GW}, e, q_{\rm BH})\,\sigma^{3.7}$ (see eq. [4.8]) computed for $\alpha = 2.63$, $q_{\rm BH} = 1$, $e = 0$ ($e = 0.99$) and $t_{\rm GW} = 10^9 - 10^8 - 10^7 - 10^6$ yr (from top to bottom). The red strip is computed using equation (4.8) for only the gaseous component, assuming $E_{\rm iso,gas} = 0.1\,E_{\rm iso,bulge}$.

energy dissipation (making the binary more and more eccentric until $e \to 1$), the energy input from the BH binary may have two main effects: (i) to modify the thermal and density structure of the grand disc; (ii) to halt the BH binary hardening (by "evaporating" the environment) before gravitational wave emission intervenes to guide the BHs toward coalescence. This "negative" feedback on the BH binary fate may indeed cause the "stalling" of the binary, a problem that has been discussed mainly in the context of pure stellar backgrounds (e.g. Merritt 2006a).

In this section we would like to introduce a simple argument based on energy conservation (i.e., assuming that angular momentum transport is accompanied by some energy dissipation) in the attempt to investigate whether the BH binary deposits enough energy to modify its surroundings and influence its fate.

Thus, consider a BH binary of total mass $M_{\rm BH}$, reduced mass $\mu_{\rm BH}$, and mass ratio $q_{\rm BH}$. The binary will coalesce in a time $t_{\rm GW}$ under the action of gravitational wave emission if its semi-major axis a is smaller than

$$a_{\rm GW} = \left(\frac{256}{5}\frac{G^3}{c^5} f(e) M_{\rm BH}^2 \mu_{\rm BH} t_{\rm GW}\right)^{1/4}, \qquad (4.1)$$

where $f(e) = [1 + (73/24)e^2 + (37/96)e^4](1-e^2)^{-7/2}$ (note that as $e \to 1$, $a_{\rm GW} \to \infty$).

This separation is of only 8×10^{-4} pc if we consider a BH binary of total mass $10^6\,\mathrm{M}_\odot$, with eccentricity $e = 0$, mass ratio $q_{\rm BH} = 1$, and merging time of $t_{\rm GW} = 10^9$ yr.

If the BH are initially unbound (as it is the case of a galaxy merger) the total energy $\Delta E_{\rm BBH}$ that the BH binary needs to deposit in its environment to reach $a_{\rm GW}$ is

$$\Delta E_{\rm BBH} = \frac{1}{2}\left(\frac{256}{5}\frac{G^3}{c^5}f(e)\right)^{-1/4} G M_{\rm BH}^{5/4}\frac{q_{\rm BH}^{3/4}}{(1+q_{\rm BH})^{3/2}} t_{\rm GW}^{-1/4}. \tag{4.2}$$

For the binary considered

$$\Delta E_{\rm BBH} \approx 1.3\times 10^{55}\left(\frac{M_{\rm BH}}{10^6\,\mathrm{M}_\odot}\right)^{5/4}\left(\frac{10^9\mathrm{yr}}{\mathrm{t_{GW}}}\right)^{1/4}\quad \mathrm{erg}. \tag{4.3}$$

If we simply model the binary environment with an isothermal sphere of effective radius $R_{\rm e}$, mass $M_{\rm iso}$ and 1-D velocity dispersion σ, BH coalescence imposes, as necessary condition

$$\Delta E_{\rm BBH} < E_{\rm iso}, \tag{4.4}$$

where $E_{\rm iso} = M_{\rm iso}\sigma^2$ is the binding energy of the isothermal sphere. An energy $\Delta E_{\rm BBH}$ of the order of $E_{\rm iso}$ would modify the equilibrium structure of the sphere and halt binary decay. If we identify the sphere with the stellar "bulge" hosting the BH binary, and write $M_{\rm iso,bulge} = \mathcal{K}\sigma^\alpha$, binary coalescence is possible if

$$\frac{1}{2}\frac{G\mu_{\rm BH}M_{\rm BH}}{a_{\rm GW}} < \mathcal{K}\sigma^{\alpha+2}. \tag{4.5}$$

Then, using the Fundamental Plane relation (Cappellari et al. 2006) and the mass–to–light ratio as in Zibetti et al. (2002), the bulge mass can be expressed as

$$M_{\rm bulge} \approx 1.54\times 10^{11}\left(\frac{\sigma}{200\,\mathrm{km\,s^{-1}}}\right)^{2.63}\mathrm{M}_\odot, \tag{4.6}$$

and an approximate estimate to the binding energy is

$$E_{\rm iso,bulge} \approx \times 10^{59}\left(\frac{\sigma}{200\,\mathrm{km\,s^{-1}}}\right)^{4.63}\mathrm{erg}. \tag{4.7}$$

Equation (4.5) combined with (4.2) then results in an upper limit for the binary BH mass

$$M_{\rm BH} < M_{\rm BH}^{\rm max} \equiv \mathcal{M}(t_{\rm GW}, e, q_{\rm BH})\sigma^{4(\alpha+2)/5}; \tag{4.8}$$

above $M_{\rm BH}^{\rm max}$ the energy deposited by the binary in its hardening would become comparable to the binding energy of the surrounding and coalescence would be halted.

$M_{\rm BH}^{\rm max}$ depends on σ and, for our choice of α, $M_{\rm BH}^{\rm max} \propto \sigma^{3.7}$ while its normalization $\mathcal{M}$ is fixed by the coefficient $\mathcal{K}$ and by the parameters intrinsic to the binary, i.e., $t_{\rm GW}$, e, and mass ratio $q_{\rm BH}$. For $t_{\rm GW}$ between 10^6 yr and 10^9 yr, $e = 0$, and $q_{\rm BH} = 1$, the values of $M_{\rm BH}^{\rm max}$ are inferred from equations (4.6) and (4.8), and plotted in Figure 12 in black colors. In the plane $M_{\rm BH}$–σ we overlaid the BH masses from Tremaine et al. (2002) for a comparison with the observations. If the observed BH masses in the sample of Tremaine are the result of a BH binary merger that led also to the formation of the host elliptical, we then conclude that BH binary coalescences did not affect the equilibrium structure of the bulges. If we consider very eccentric ($e = 0.99$) equal mass binaries, equations (4.6) and (4.8) leads to upper mass limits (depicted with the blue strip) again well above the observed points, thus providing less stringent constraints on the BH binary fate. Unequal mass binaries move further upwards, on the left side of the diagram.

The decaying BH binary have thus no effect on the overall stellar bulge. However, they

can have some influence inside the bulge, in a region much larger than the gravitational influence radius of a "single" BH, defined as

$$r_{\rm BH} = GM_{\rm BH}/\sigma^2. \tag{4.9}$$

Since the mass within radius r of an isothermal sphere scales as $M_{\rm iso}(r) = 2\,r\,\sigma^2/G$ we can determine the "radius of BH binary gravitational influence", $r_{\rm BBH}$, obtained by equating $\Delta E_{\rm BBH}$ to the energy inside $r_{\rm BBH}$, i.e., $\Delta E_{\rm BBH} = M_{\rm iso}(r_{\rm BBH})\sigma^2$:

$$r_{\rm BBH} = \frac{1}{4}\left(\frac{256}{5}\frac{G^3}{c^5}f(e)\right)^{-1/4}\frac{q_{\rm BH}^{3/4}}{(1+q_{\rm BH})^{3/2}}t_{\rm GW}^{-1/4}\left(\frac{G^2M_{\rm BH}^{5/4}}{\sigma^4}\right). \tag{4.10}$$

This radius is considerably larger than $r_{\rm BH}$. For a $10^8\,{\rm M}_\odot$ equal mass–circular BH binary $r_{\rm BBH}/r_{\rm BH} \approx 25$, assuming $\sigma \sim 200\,{\rm km\,s^{-1}}$. The above relation may thus account for the size of the stellar core seen in the bright elliptical galaxies as extensively discussed by Merritt (2006b).

If the bulge hosts a gaseous nuclear component, the energy released by the binary during its path to coalescence may alter the equilibrium of the surrounding gas and a delicate interplay between heating/cooling of the gas and hardening of the binary may lead to a "self-regulated" evolution of the BH mass and the circum–binary gas. Given the expected widespread values of $E_{\rm iso,gas}$ for a nuclear gaseous component in merging galaxies, due to diversities in the mass gas content, thermodynamics and equilibrium end–states, we simply rescale $E_{\rm iso,gas} = 0.1E_{\rm iso,bulge}$ and plot the corresponding red strip in Figure 12, for $e = 0$, $q_{\rm BH} = 1$ and same interval of merging times ($t_{\rm GW} = 10^6 - 10^9$ yr). The strip now shifts to the right and gets closer to the BHs observed along the $M_{\rm BH}$–σ relation. For $t_{\rm GW}$ less than 10^7 yr, there are uncloalesced BHs and BHs that may have deposited enough energy to affect the surrounding gas. This point will be addressed in future investigations.

A further energy constraint may come from accretion. First notice that the gravitational wave time scale $t_{\rm GW}$ is here treated as a parameter. However in the nuclear region of the galaxy its value is determined by the mechanisms guiding the inspiral, i.e., material (viscous) and gravitational torques and energy dissipation via shocks and radiation. We know that viscosity is the critical parameter at the heart of BH binary hardening on sub–parsec scales (Armitage & Natarajan, 2002), and at the heart of accretion (fixing the magnitude of the mass transfer rate toward the BHs). As shown in Section 3.4, gas inflows, after orbit circularization, may trigger AGN activity onto the BHs, at least temporary, and a stringent condition for BH binary coalescence, in this context, may come from the request that the difference between the energy deposited by the accreting BHs in the gas and the energy radiated away by cooling processes (here denoted as $\Delta E_{\rm acc}$) be less that the binding energy of the gas itself (denoted with $E_{\rm iso,gas}$, here for simplicity):

$$\Delta E_{\rm acc} \sim f_{\rm acc}\left(\frac{L}{L_E}\right)\left(\frac{t}{t_{\rm Edd}}\right)\epsilon M_{\rm BH}c^2 < E_{\rm iso,gas} \tag{4.11}$$

(with L_E the Eddington luminosity and $f_{\rm acc}$ the fractional energy deposited by the accreting BH in the surrounding gas). Typically

$$\Delta E_{\rm acc} \approx 2\times 10^{59} f_{\rm rad}\left(\frac{L}{L_E}\right)\left(\frac{t}{t_{\rm Edd}}\right)\left(\frac{\epsilon}{0.1}\right)\left(\frac{M_{\rm BH}}{10^6\,{\rm M}_\odot}\right){\rm erg}. \tag{4.12}$$

This energy can be larger than $\Delta E_{\rm BBH}$, and may be comparable to the binding energy of the environment, indicating that a major threat to BH binary stalling in a gaseous background might come from the radiative and/or mechanical energy emitted by the accret-

ing BHs during their inspiral and hardening. Only short–lived (i.e., $t_{\rm GW} < t_{\rm Edd}$), and/or sub-Eddington accretion can guarantee the persistence of a "dense and cool" gaseous structure around the binary. Modeling of realistic nuclear discs will help in quantifying accurately $E_{\rm iso,gas}$ and the problem of the BH hardening in a gaseous environment (Colpi et al. in preparation).

5. Summary

• In gas-rich galaxy–galaxy collisions, the BHs "pair" first under the action of dynamical friction against the dark matter background. When the merger is sufficiently advanced that tidal forces have perturbed the gaseous/stellar discs of the mother galaxies, each BH is found to be surrounded by a prominent gaseous disc. The BHs have now separations of several kiloparsecs.

• When the merger is completed, a rotationally supported, turbulent, nuclear gaseous disc forms at the center of the remnant galaxy. In this "grand" disc of $\sim 19^9$ $M_\odot$, the BHs excite large scale density waves: gas–dynamical friction is the main driver of their inspiral down to the parsec–scale. A few million years after the completion of the merger the BHs "couple" to form an eccentric *Keplerian binary*. The binary is embedded in the typical, cool environment of a starburst.

• The binary eccentricity decreases to zero if the BHs bind, in the grand disc, along a co–rotating orbit. It remains large ($e > 0$), if the BHs bind along counter–rotating orbits. However, this effect may not be generic: in presence of a very massive nuclear disc with steep density profile, asymmetric instabilities growing in the innermost self-gravitating region could in principle exert torques on the binary, increasing its eccentricity. The evolution of e is thus sensitive to the dynamical pattern of the gas surrounding the binary.

• If the binary circularizes, a small-scale accretion disc forms around each BH, and double AGN activity can be sustained for approximately 1 Myr, on scales less than 10 parsecs.

• No compelling evidence exists on the actual fate of the BH binary in a gaseous environment: whether it stalls or keep decaying under the action of gravitational and viscous torques until gravitational wave emission guides the inspiral toward coalescence. This may depend sensitively on the BH mass, mass ratio, eccentricity, and thermodynamical response of the gaseous environment to the BH perturbation. We note here that a possible threat may come from energy injection by the BHs, should they accrete, or/and (to a lesser extent) from the energy extracted from the orbit and deposited in the surroundings.

REFERENCES

Arena, S. E., & Bertin, G., 2007 Slow evolution of elliptical galaxies induced by dynamical friction. III. Role of density concentration and pressure anisotropy. *A&A* **463**, 921

Armitage, P. J., & Natarajan, P., 2002 Accretion during the merger of supermassive black holes. *Astrophys. J.* **567**, 9

Ballo, L., Braito, V., Della Ceca, R., Maraschi, L., Tavecchio, F., Dadina, M., 2004 Arp 299: a second merging system with two active nuclei? *Astrophys. J.* **600**, 634

Bate, M. R., & Burkert, A., 1997 Resolution requirements for smoothed particle hydrodynamics calculations with self-gravity. *Mon. Not. R. Astron. Soc.* **288**, 106

Begelman , M. C., Blandford, R. D., & Rees, M. J., 1999 Massive black hole binaries in active galactic nuclei. *Nature* **287**, 307

Bender, P. et al. 1994 Laser Interferometer Space Antenna for gravitational waves measurements: ESA assesment study report. *ESA Report*

Berczik, P., Merritt, D., & Spurzem, R., 2005 Long-Term Evolution of Massive Black Hole Binaries. II. Binary Evolution in Low-Density Galaxies. *Astrophys. J.* **633**, 680

Cappellari, M., et al. 2006 The SAURON project - IV. The mass-to-light ratio, the virial mass estimator and the Fundamental Plane of elliptical and lenticular galaxies. *Mon. Not. R. Astron. Soc.* **366**, 1126

Colpi, M., Mayer, L., & Governato, F., 1999 Dynamical friction and the evolution of satellites in virialized halos: the theory of linear response. *Astrophys. J.* **525**, 720

Colpi, M., Callegari, S., Dotti, M., Kazantzidis, S., & Mayer, L., 2007 On the inspiral of massive black holes in gas–rich galaxy mergers. *P*roceedings of the Conference "The multicoloured landscape of compact objects and their explosive origins", Cefalu 2006 **arXiv:0706.1851**

Della Ceca, R., et al. , 2002 An Enshrouded Active Galactic Nucleus in the Merging Starburst System Arp 299 Revealed by BeppoSAX. *Astrophys. J.* **581**, 9

Di Matteo, T., Colberg, J., Springel, V., Hernquist, L., & Sijacki, D., 2007 Direct cosmological simulations of the growth of black holes and galaxies. *Submitted to Astrophys. J.* arXiv:0705.2269

Di Matteo, T., Springel, V., & Hernquist, L., 2005 Energy input from quasars regulates the growth and activity of black holes and their host galaxies. *Nature* **433**, 604

Dotti, M., Colpi, M., & Haardt, F., 2006 Laser Interferometer Space Antenna double black holes: dynamics in gaseous nuclear discs. *Mon. Not. R. Astron. Soc.* **367**, 103

Dotti, M., Colpi, M., Haardt, F., & Mayer, L., 2007 Supermassive black hole binaries in gaseous and stellar circumnuclear discs: orbital dynamics and gas accretion. *Mon. Not. R. Astron. Soc.* **379**, 956.

Downes, D., & Solomon, P. M., 1998 Rotating nuclear rings and extreme starbursts in ultraluminous galaxies. *Astrophys. J.* **507**, 615

Escala, A., Larson, R. B., Coppi, P. S., & Maradones, D., 2004 The role of gas in the merging of massive black holes in galactic nuclei. I. black hole merging in a spherical gas cloud. *Astrophys. J.* **607**, 765

Escala, A., Larson, R. B., Coppi, P. S., & Maradones, D., 2005 The role of gas in the merging of massive black holes in galactic nuclei. II. Black hole merging in a nuclear gas disk. *Astrophys. J.* **630**, 152

Ferrarese, L., & Merritt, D., 2000 A fundamental relation between supermassive black holes and their host galaxies. *Astrophys. J.* **539**, 9

Gebhardt, K, et al. , 2000 A relationship between nuclear black hole mass and galaxy velocity dispersion. *Astrophys. J.* **543**, 5

Gould, A., & Rix, H., 2000 Binary black hole mergers from planet-like migrations. *Astrophys. J.* **532**, 29

Governato, F., Colpi, M., & Maraschi, L. 1994 The fate of central black holes in merging galaxies. *Mon. Not. R. Astron. Soc.* **271**, 317

Graham, A. W., & Driver, S. P. 2007 A log-quadratic relation for predicting supermassive black hole masses from the host bulge Sersic index. *Astrophys. J.* **655**, 77

Granato, G.L., De Zotti, G., Silva, L., Bressan, A., Danese L. 2004 A phyisical model for the coevolution of QSOs and their spheroidal hosts. *Astrophys. J.* **600**, 580

Gualandris, A., & Merritt, D., 2007 Dynamics around supermassive black holes. *To appear in "2007 STScI Spring Symposium: Black Holes", eds. M. Livio & A. M. Koekemoer. (Cambridge University Press, in press)* (arXiv:0708.3083)

Haehnelt, M. G., 1994 Low-frequency gravitational waves from supermassive black-holes. *Mon. Not. R. Astron. Soc.* **269**, 199

Hernquist, L., 1993 N-body realizations of compound galaxies. *Astrophys. J. Supp.* **86**, 389

Jaffe, A. H., & Backer, D. C., 2003 Gravitational waves probe the coalescence rate of massive black hole binaries. *Astrophys. J.* **583**, 616

Katz, N., 1992 Dissipational galaxy formation. II - Effects of star formation. *Astrophys. J.* **391**, 502

Kaufmann, T., Mayer, L., Wadsley, J., Stadel, J., & Moore, B., 2006 Cooling flows within galactic haloes: the kinematics and properties of infalling multiphase gas. *Mon. Not. R. Astron. Soc.* **370**, 1612

Kazantzidis, S., et al. 2005 The Fate of Supermassive Black Holes and the Evolution of the $M_{\rm BH}$–σ Relation in Merging Galaxies: The Effect of Gaseous Dissipation. *Astrophys. J.* **623**, 67

Khochfar, S., & Burkert, A., 2006 Orbital parameters of merging dark matter halos. *A & A* **445**, 403

King, A. R., 2003 Black holes, galaxy formation, and the $M_{\rm BH}$–σ relation. *Astrophys. J.* **596**, 27

Kitsionas, S., & Whitworth, A. P., 2002 Smoothed Particle Hydrodynamics with particle splitting, applied to self-gravitating collapse. *Mon. Not. R. Astron. Soc.* **330**, 129

Klessen, R. S., Spaans, M., Jappsen, A., 2007 The stellar mass spectrum in warm and dusty gas: deviations from Salpeter in the Galactic centre and in circumnuclear starburst regions. *Mon. Not. R. Astron. Soc.* **374**, 29

Klypin, A., Zhao, H., & Somerville, R. S. 2002 CDM-based Models for the Milky Way and M31. I. Dynamical Models. *Astrophys. J.* **573**, 597

Komossa, S. 2006 Observational evidence for binary black holes and active double nuclei. *Memorie della Societa Astronomica Italiana* **77**, 733

Komossa, S., Burwitz, V., Hasinger, G., Predehl, P., Kaastra, J. S., & Ikebe, Y. 2003 Discovery of a binary active galactic nucleus in the ultraluminous infrared galaxy NGC 6240 using Chandra. *Astrophys. J.* **582**, 15

Kormendy, J., & Richstone, D., 1995 Inward bound - the search for supermassive black holes in galactic nuclei. *ARA&A* **33**, 581

Magorrian, et al. 1998 The demography of massive dark objects in galaxy centers. *Astron. J.* **115**, 2285

Makino, J., & Ebisuzaki, T., 1996 Merging of Galaxies with Central Black Holes. I. Hierarchical Mergings of Equal-Mass Galaxies. *Astrophys. J.* **465**, 527

Makino, J., & Funato, Y., 2004 Evolution of Massive Black Hole Binaries. *Astrophys. J.* **602**, 93

Max, C., E., Canalizo, G., & de Vries, W. H., 2007 Locating the two black holes in NGC 6240. *Science* **316**, 1877

Mayer, L., Kazantzidis, S., Madau, P., Colpi, M., Quinn, T., Wadsley, J., 2007 Rapid formation of supermassive black hole binaries in galaxy mergers with gas. *Science* **316**, 1874

Merritt, D., 2006a Dynamics of galaxy cores and supermassive black holes. *Rept.Prog.Phys.* **69**, 2513

Merritt, D., 2006b Mass deficits, stalling radii, and the merger histories of elliptical galaxies. *Astrophys. J.* **648**, 976

Milosavljevic, M., Merritt, D., 2001 Formation of Galactic Nuclei. *Astrophys. J.* **563**, 34

Navarro, J. F., Frenk, C. S., & White, S. D. M., 1996 The Structure of Cold Dark Matter Halos. *Astrophys. J.* **462**, 563

Ostriker, E. C., 1999 Dynamical friction in a gaseous medium. *Astrophys. J.* **513**, 252

Richstone, D., 1998 Supermassive black holes and the evolution of galaxies. *Nature* **395**, 14

Rodriguez, C., Taylor, G. B., Zavala, R. T., Peck, A. B., Pollack, L. K., & Romani, R. W., 2006 A compact supermassive binary black hole system. *Astrophys. J.* **646**, 623

Sanchez-Salcedo, F. J., & Brandenburg, A., 2001 Dynamical friction of bodies orbiting in a gaseous sphere. *Mon. Not. R. Astron. Soc.* **322**, 67

Sesana, A., Haardt, F., Madau, P., & Volonteri, M. 2005 The gravitational wave signal from massive black hole binaries and its contribution to the LISA data stream. *Astrophys. J.* **623**, 23

Sesana, A., Haardt, F., & Madau, P., 2007 Interaction of massive black hole binaries with their stellar environment. II. Loss cone depletion and binary orbital decay. *Astrophys. J.* **660**, 546

Silk, J., & Rees, M. J., 1998 Quasars and galaxy formation. *A&A* **331**, 1

Spaans, M., & Silk, J., 2000 The Polytropic Equation of State of Interstellar Gas Clouds. *Astrophys. J.* **538**, 115

Springel, V., Di Matteo, T., Hernquist, L., 2005 Modelling feedback from stars and black holes in galaxy mergers. *Mon. Not. R. Astron. Soc.* **361**, 776

Springel, V., Di Matteo, T., Hernquist, L., 2005 Black holes in galaxy mergers: the formation of red elliptical galaxies. *Astrophys. J.* **620**, 79

Springel, V., Frenk, C. S., White, S. D. M., 2006 The large-scale structure of the Universe. *Nature* **440**, 1137

Springel, V., & Hernquist, L., 2003 Cosmological smoothed particle hydrodynamics simulations: a hybrid multiphase model for star formation. *Mon. Not. R. Astron. Soc.* **339**, 289

Springel, V., Yoshida, N., & White S. D. M., 2001 GADGET: a code for collisionless and gasdynamical cosmological simulations. *New Astron.* **6**, 79

Tremaine, S., et al. , 2002 The slope of the black hole mass versus velocity dispersion correlation. *Astrophys. J.* **574**, 740

Vecchio, A. 2004 LISA observations of rapidly spinning massive black hole binary systems. *Phys. Rev. Letts.* **70**, 2001

Vitale, S. et al., 2002 LISA and its inflight test precursor SMART-2. *Nuclear Physics B; Proceeding Supplements* **110**, 209

Volonteri, M., Haardt, F., & Madau, P., 2003 The assembly and merging history of supermassive black holes in hierarchical models of galaxy formation. *Astrophys. J.* **582**, 559

Wadsley, J., Stadel, J., & Quinn, T., 2004 Gasoline: a flexible, parallel implementation of TreeSPH. *New Astr.* **9**, 137

Yu, Q., 2002 Evolution of massive binary black holes. *Mon. Not. R. Astron. Soc.* **331**, 935

Zibetti, S., Gavazzi, G., Scodeggio, M., Franzetti, P., & Boselli, A., 2002 1.65 micron (H band) surface photometry of galaxies. X. Structural and dynamical properties of elliptical galaxies. *Astrophys. J.* **579**, 261